# Modulate Siglec-7 Signaling via *in situ* Created High-affinity *cis*-Ligands

Senlian Hong[1], Chenhua Yu[1,2], Yujie, Shi[1], Peng Wang[1], Digantkumar G. Chapla[3], Emily Rodrigues[4], Kelly W. Moremen[3], James C. Paulson[1], Matthew S. Macauley[4], and Peng Wu[1,*]

[1]Department of Molecular Medicine, The Scripps Research Institute, La Jolla, California, 92037, U. S. A.

[2]School of Medicine, Nankai University, Tianjin 300071, China.

[3]Complex Carbohydrate Research Center, University of Georgia, Athens, Georgia, 30602, U. S. A.

[4]Departments of Chemistry, Medical Microbiology and Immunology, University of Alberta, 11227 Saskatchewan Dr NW, Edmonton, AB T6G 2G2, Alberta, Canada.

*Correspondence: pengwu@scripps.edu (P.W.)

**Abstract**

Sialic acid-binding immunoglobulin-like lectins, also known as Siglecs, have recently been designated as glyco-immune checkpoints. Through their interactions with sialylated glycan epitopes overexpressed on tumor cells, inhibitory Siglecs expressed on innate and adaptive immune cells modulate signaling cascades to restrain anti-tumor immune responses. However, the mechanisms underlying these processes are just started to be elucidated. We discover that when human natural killer (NK) cells attack tumor cells, glycan remodeling occurs in the target cells at the immunological synapse. This remodeling occurs through both transfer of sialylated glycans from NK cells to target tumor cells and accelerated *de novo* synthesis of sialosides on the tumor cells. Functionalization of NK cells with a high-affinity ligand of Siglec-7 leads to multifaceted roles in modulating Siglec-7-regulated NK activation. At high levels, the added Siglec-7 ligand suppresses NK cytotoxicity through the recruitment of Siglec-7, whereas at low levels the same ligand triggers the release of Siglec-7 from the cell surface into the culture medium, preventing Siglec-7-mediated inhibition of NK cytotoxicity. These results suggest that glycan engineering of NK cells may provide a means to boost the NK activity for cancer treatment.

## Introduction

The development of immune checkpoint inhibitors for blocking the suppressive functions of cytotoxic T-lymphocyte-associated protein 4 (CTLA-4) and programmed cell death protein 1 (PD-1) has offered curative hopes for many cancer patients.[1-3] Upon checkpoint blockade treatments, remarkable tumor regression and significant survival benefits for patients with a broad spectrum of advanced cancers have been observed clinically. However, more than 50% of cancer patients fail to respond to such treatments,[2] suggesting the existence of other immune checkpoints that are orthogonal to the above well-established ones. Recently, the Siglecs (sialic acid–binding immunoglobulin-like lectins) family of sialic acid binding proteins has been designated as glyco-immune checkpoints.[4-8] Through their interaction with sialylated glycan epitopes aberrantly expressed on tumor cells, inhibitory Siglecs such as Siglec-7 and -9 that are found on innate immune cells, e.g. natural killer cells, inhibit immune signaling pathways to restrain immune-system activation.[6,7,9-11] Likewise, Siglec-15 upregulated on tumor cells interact with yet-to-be identified T-cell membrane glycoproteins to suppress T cell anti-tumor functions.[5] Despite these exciting discoveries that correlate Siglec-mediated immune suppression to cancer progression, we have a poor understanding of the prevalence of the Siglec-ligand expression. Moreover, the mechanisms that governs Siglec-ligand-interaction-mediated immune suppression is only partially elucidated.[7,12,13]

When Siglec-7 or -9 expressing NK cells encounter their target tumor cells, binding to *trans* ligands expressed by tumor cells recruits these Siglecs to the immune synapse, where their immunoreceptor tyrosine-based inhibition motifs (ITIMs) are phosphorylated by Src kinase, thereby creating a binding site for the tyrosine phosphatases SHP-1 and SHP-2.[8,9,14] Binding of SHP-1/2 leads to de-phosphorylation of signaling components downstream of activation receptors to suppress NK cell activation and effector function. Therefore, it seems reasonable to postulate that tumor cells express higher levels of Siglec ligands to counteract NK-induced killing. However, when surveying tumor specimens and matched normal tissues, we unexpectedly discovered that high Siglec-7 ligand expression was found in both normal and malignant tissues. Here, we report that when live cancer cells encounter NK cells, a significant upregulation of Siglec-7 ligands is detected within one hour, suggesting that this inhibitory pathway may serve as a negative feedback mechanism that follows NK cell infiltration. Using sialyltransferase-mediated chemoenzymatic glycan editing, a high-affinity Siglec-7 ligand could be newly created on NK cells directly. Introducing such a ligand, in *cis*, induces multifaceted effects on Siglec-7 signaling and NK effector function.

## Sialylated glycans protect cancer cells from NK cytotoxicity through the interaction with Siglec-7 on NK cells

To understand how the interactions between Siglec-7 and its sialic acid ligands on cancer cells are involved in modulating NK cell-mediated tumor cell killing, we first assessed the expression of Siglec-7 ligands on a panel of cancer cell lines and primary human immune cells using a recombinant Siglec-7 Fc chimera by flow cytometry. Among the cancer cell lines that we screened, Raji B lymphoma and MDA-MB-435 melanoma cells were found to possess the highest level of Siglec-7 ligand (Figure 1a), whereas prostate cancer cell line LNCap and several ovarian and colorectal cancer cell lines only showed basal levels of Siglec-7 ligands. Although only basal levels of Siglec-7 ligands were found on vascular endothelial cell line HUVEC, freshly isolated NK cells, peripheral blood mononuclear cells (PMBCs), and activated T cells expressed abundant levels of Siglec-7 ligands. To assess *in situ* expression of Siglec-7 ligands, we analyzed paraffin-embedded human tumor and adjacent tissue specimens from a number of malignancies. Significant Siglec-7 Fc staining was detected in almost all specimens analyzed (Figure 1b-d, Supplementary figure s1, and s2); both primary tumor and the matched adjacent tissue specimens exhibited different levels of Siglec-7 Fc staining, which was abolished upon neuraminidase treatment (Figure 1b and 1c). In particular, we examined 177 specimens from lung cancer patients and 20 specimens from normal lung tissues (Figure 1d, 1e and Supplementary figure s2), and found that approximately 20–40% of lung cancer tissues and 85% of normal lung tissues expressed high levels of Siglec-7 ligands. These observations demonstrate that Siglec-7 ligands are uniquely found on cancer tissues, suggesting that their presence may not be a reliable marker for cancer detection.

**Desialylation of target cancer cells expressing Siglec-7 ligands enhances NK-cell effector functions**

Due to the high expression of Siglec-7 ligands on Raji cells, we used these cells as the target (T) cells to determine the impact of the interaction between Siglec-7 on NK cells and cancer cell-expressed Siglec-7 ligands on NK-cell effector functions. Primary NK cells[15,16] isolated from periphery blood of healthy donors and NK-92MI cells[17,18] were used as sources of NK effector (E) cells.

NK cells isolated from healthy donors were expanded in culture with interleukin 2 (IL2) and IL15 for 10 days to generate a large number of cells for in *vitro* functional evaluation (these NK cells were defined as peripheral NK cells). The freshly isolated peripheral NK cells contained approximately 40%~60% of Siglec-7 positive cells, and the frequency of this subset decreased slightly after 10-day *in vitro* culture (Supplementary figure s3). Consistent with previous reports,[19,20] culture with interleukin 2 (IL2) and IL15 significantly improved the cytotoxicity of periphery NK cells towards Raji cells (Supplementary figure s3c). To assess the NK-induced target cell killing, we incubated target Raji cells with peripheral NK cells for 4h and determined the target cell killing using a lactate dehydrogenase release assay. As shown in Figure 2a, NK-induced target-cell-killing was enhanced along with increasing the effector cell-to-target cell ratio (E/T ratio). Pre-desialylation of Raji cells by neuraminidase significantly enhanced their susceptibility to the NK-induced killing. Similarly, enhanced Raji cell killing was observed when the Siglec-7 functional blocking antibody s7.7[8] was used.

Next, we assessed target cell killing using NK-92MI cells, a constantly cytotoxic NK cell line currently undergoing clinical trials as an 'off-the-shelf therapeutic' for treating both hematological and solid malignancies.[17,18] NK-92MI cells were originally derived from a CD56$^{bright}$-NK population,[21] only a small subset (~10%) of which expressed Siglec-7 (we define this status as NK-92MI-S7$^{low}$). With increased passages in media supplemented with non-heat-inactivated horse serum, Siglec-7 positive subset became the dominant subset. After approximately 120 days in culture, ~90% NK-92MI became Siglec-7 positive (we define this status as NK-92MI-S7$^{high}$) (Supplementary figure s4). As expected, compared to NK-92MI-S7$^{low}$ cells, NK-92MI-S7$^{high}$ cells induced approximately 55% reduced killing of Raji cells (E/T ratio = 5:1) (Figure 2b). The NK-92MI-S7$^{high}$-associated cytotoxicity could be enhanced by the Siglec-7 blocking antibody (s7.7) that blocks the ability of Siglec-7 to bind its glycan ligands or by pre-desialylation of Raji cells. Increased IFN-λ and granzyme B secretions were also in response to abrogated Siglec-7 ligand interactions (Figure 2c). The same treatments also increased the cytotoxicity of NK-92MI-S7$^{low}$ cells but to a much lesser degree (Figure 2b). Similar results were observed by using Daudi cells that express moderate levels of Siglec-7 ligands as the target cells (Supplementary figure s5). Together, these results were consistent with what was reported by Démoulins and Bertozzi previously,[6,7] and strongly indicate that Siglec-7 ligands on cancer cells protect them from NK cytotoxicity via interaction with Siglec-7 on NK cells.

**Interactions between NK and cancer cells leads to an upregulation of Siglec-7 ligands on tumor cells**

During the course of monitoring interactions between Raji and NK-92MI or periphery NK cells, we observed a significant increase of sialylated glycans on their cell surface within 2 hours, as revealed by lectin staining with *Sambucus nigra* lectin (specific for α2-6-sialosides) and *Maackia Amurensis* lectin II (specific for α2-3-sialosides) (Figure 3a-c, and Supplementary figure s6). We considered several possibilities through which Raji cells could elevate their surface sialylated glycans: (1) transfer of sialylated glycoconjugates from NK cells, (2) an increase in *de novo* sialic acid synthesis, and/or (3) reduced endocytosis on Raji cell. To examine the first possibility and determine if sialosides on Raji cells were transferred from NK cells, NK cells were cultured in the presence of peracetylated *N*-(4-pentynoyl)mannosamine ($Ac_4$ManNAl)[22] to metabolically incorporate an alkyne-containing Neu5Ac (SiaNAl) onto cell surface glycoconjugates. After 48h, NK cells with newly synthesized sialosides labeled by SiaNAl were incubated with Raji cells for 1.5h and the cell mixture was reacted with biotin-azide via the ligand (BTTPS)-assisted copper-catalyzed azide-alkyne [3+2] cycloaddition reaction (CuAAC)[23], followed by flow cytometry analysis. A robust biotinylation signal was detected on NK cells that were cultured with $Ac_4$ManNAl. Upon incubating with Raji cells, a 40% decrease in the NK-

associated biotin signal was observed, along with the appearance of the biotin signal on Raji cells, suggesting that alkyne-tagged sialic acids were transferred from NK to Raji calls (Figure 3d and 3e).

We next examined the second and third possibility, whether there was increased *de novo* sialic acid synthesis and/or reduced endocytosis on Raji cells upon NK cell encountering, respectively. Raji cells were metabolically labelled with $Ac_4$ManNAl for 48h and subjected to the CuAAC-mediated biotin conjugation before and after incubation with NK-92MI cells. In comparison to Raji cells without prior NK incubation, Raji cells that were incubated with NK cells exhibited a 2fold higher biotinylation signal (Figure 3f and 3g). It is noteworthy that the endogenously increased sialylation was at least 200-fold higher than that transferred from NK cells (compare MFI of 400 to 90,000, shown in Figure 3e and 3g). Importantly, the increased SiaNAl incorporation on the cell surface was largely blocked by Brefeldin A[24], which inhibits protein transport from the endoplasmic reticulum to the Golgi complex, but not by the endocytic inhibitor Dynasore[25] (Figure 3g). Similarly, co-incubation of Raji cells with periphery NK cells also triggered a quick accumulation of newly synthesized sialylation, which in turn significantly augmented sialylation on Raji cell surface (Figure 3h). Notably, no obvious transfer of sialic acids from Raji to NK cells was observed. As a consequence of the increased Raji cell-surface sialylation, a notable elevation of Siglec-7 Fc binding was detected (Figure 3i). In addition, Siglec-7-specific blocking antibody did not prevent the increase of Raji cell-surface sialylation, suggesting that Siglec-7 may not be involved in triggering this process (Supplementary figure s7). In parallel, we examined if incubating HEK293T cells, a cell line derivate from human embryonic kidney cells, with NK cells could increase their cell-surface sialylation levels as what we had observed for malignant cells. We found that HEK293T cells were not attacked by NK cells (Supplementary figure s8). However, upon NK encountering, a modest up-regulation of cell-surface sialylation was detected, and the up-regulated sialic acid was derived primarily from NK cell surface rather than *de novo* synthesized (Supplementary figure s8e). Together, the above observations suggest that interactions with NK cells leads to sialoside transfer from NK cell to the encountering cells. However, d*e novo* sialylated glycan biosynthesis is only induced when the killing of the encountering cells is triggered.

Subsequently, we sought to determine if there is any correlation between NK cell infiltration into tumor tissues and the *in situ* expression of Siglec-7 ligands. We analyzed paraffin-embedded human tumor and adjacent tissue specimens from lung malignancies by using the human NK marker CD56 and Siglec-7 Fc staining. The NK density was found to have a modest negative correlation with the Siglec-ligand expression in healthy lung tissue samples ($R^2$=0.59), whereas a weak positive correlation existed between NK infiltration and the Siglec-ligand expression in malignant lung tissues ($R^2$=0.15 ) (Supplementary figure s9), suggesting that the up-regulation of Siglec-7 ligands may be triggered by NK cell infiltration into tumor tissues.

**Engineering glycocalyx of NK cells via chemoenzymatic glycan editing**

Previous studies by Crocker and coworkers revealed that Siglec-7 on the NK cell surface is masked by *cis* ligands, which partially block its interactions with *trans* ligands found on target cells.[26,27] Unmasking of Siglec-7 induces strong suppression of NK-induced tumor cell killing due to the binding of Siglec-7 with its *trans* ligands. Based on this precedent, we hypothesized that functionalizing NK cells with a high-affinity and specific ligand of Siglec-7 may further boost NK-associated cytotoxicity by preventing Siglec-7-*trans* ligand interactions. Developed by Paulson and co-workers,[28] $^{FTMC}$Neu5Ac (**2**), a chemically-functionalized version of Neu5Ac (**1**) whose C9 is substituted with 9-*N*-(1-(5-fluorescein)-1H-1,2,3-triazol-4-yl)methylcarbamate, when α2-6- or α2-3 linked to *N*-acetyllactosamine (type 2 LacNAc, Galβ1-4GlcNAc), serves as a high-affinity ligand of Siglec-7. We hypothesize that $^{FTMC}$Neu5Ac could be introduced onto NK cells via sialyltransferase-mediated chemoenzymatic glycan editing to directly create high-affinity Siglec-7 ligands in *cis* for modulating Siglec-7 signaling by preventing its interactions with *trans* ligands.

To assess this feasibility, we first synthesized CMP-$^{FTMC}$Neu5Ac (**5**) as the donor substrate. A commonly used CMP-Sia synthetase from *Neisseria meningitides* (NmCSS)[29] was not capable of directly converting $^{FTMC}$Neu5Ac to the corresponding CMP-Neu5Ac analog. Alternatively, we prepared C9-*N*-

propargyloxycarbonyl Neu5Ac (**3**, C9-$^{CPg}$Neu5Ac)[30] and converted it to CMP-C9-$^{CPg}$Neu5Ac. The resulting CMP-C9-$^{CPg}$Neu5Ac (**4**) was then reacted with 5-fluorescein azide[28] to produce CMP-$^{FTMC}$Neu5Ac (**5**) with an overall yield of ~26% (Figure 4a and Supplementary figure s18).

Chinese hamster ovary (CHO) Lec2 mutant cells[31] were used as a model system to test sialyltransferase-mediated chemoenzymatic glycan editing[32] for incorporating $^{FTMC}$Neu5Ac onto the cell surface. Lec2 cells possess relatively homogeneous peripheral N-glycans terminated with LacNAc that are capable of being modified by ST6Gal1 and ST3Gal4 to add α2-6- and α2-3-linked sialic acid, respectively (Figure 4b).[33] Because $^{FTMC}$Neu5Ac contains a fluorescein, cell-associated fluorescein fluorescence can be measured and used to quantify the number of $^{FTMC}$Neu5Ac installed. After incubating Lec2 cells with ST6Gal1 and ST3Gal4, respectively, in the presence of **5**, a dose-dependent increase of fluorescein signals was detected (Figure 4c). In control experiments, cells were treated with ST3Gal1[33] to add $^{FTMC}$Neu5Ac onto O-glycans in α2-3 linkages. When comparable levels of $^{FTMC}$Neu5Ac were installed onto the cell surface, α2-6-linked $^{FTMC}$Neu5Ac showed a significantly higher affinity to Siglec-7 than its α2-3-linked counterparts (Figure 4d). For example, whereas similar levels of fluorescein signals were detected upon treating Lec2 cells with each sialyltransferase in the presence of 10 μM CMP-$^{FTMC}$Neu5Ac, ST6Gal1-treated cells exhibited a 14-fold and 75-fold stronger Siglec-7 Fc binding than cells that were treated with ST3Gal1 and ST3Gal4, respectively. These observations indicate that Siglec-7 prefers α2-6-linked $^{FTMC}$Neu5Ac over its 2-3 linked counterparts (Figure 4c and 4d).

Next, we assessed the efficiency of ST6Gal1-mediated glycan editing on periphery NK and NK-92MI cells. Consistent with what we observed for Lec2 CHO cells, a dose- and time-dependent increase of fluorescein signals was detected upon treating NK cells with ST6Gal1 and **5** (Figure 4e, 4g, and Supplementary figure s10). When 100 μM of **5** was used for cell-surface glycan editing, Siglec-7 Fc binding reached the saturation level (Figure 4e and 4f). When <1μM of **5** was used for NK-92MI cell modification, we observed an interesting phenomenon: although comparable levels of FTMC-fluorescence could be detected on both NK-92MI Siglec-7$^{low}$ and Siglec-7$^{high}$ cells and fluorescence intensity increased along increasing dose of **5,** surprisingly, staining these two modified cells with Siglec-7 Fc chimera gave distinct results (Figure 4h). The Siglec-7 Fc staining could be detected on Siglec-7$^{low}$ cells when as low as 10 nM of **5** was used, whereas the staining above background signals on Siglec-7$^{high}$ cells was only detectable when the concentration of **5** went beyond 100 nM. This suggests that the newly installed low-concentration $^{FTMC}$Neu5Ac may be engaged in strong *cis* interactions with Siglec-7 on NK cells, which prevents its *trans* interactions with Siglec-7 Fc.

**Modulate NK-induced tumor-cell killing via a *cis* Siglec-7 ligand with high affinity**

After confirming that $^{FTMC}$Neu5Ac could be installed directly onto NK cells to form high-affinity Siglec-7 ligands, we explored the possibility of using this approach to modulate Siglec-7 immunoinhibitory signaling. To our surprise, the killing of Raji cells was significantly inhibited when NK-92MI-S7$^{high}$ cells were functionalized with $^{FTMC}$Neu5Ac when high concentration of **5** (i.e. > 100 μM) was used as the donor (Supplementary figure s11). Similar inhibition effects were also observed when desialylated target Raji and Daudi cells were used (Figure 5a and 5b). The decreased cytotoxicity of modified-NK-92MI cells toward desialylated Raji and Daudi cells was gradually rescued when the concentration of **5** used for glycan editing dropped below 1 μM. The lower the CMP-$^{FTMC}$Neu5Ac concentration became, the higher the NK-induced target cell killing. The NK cytotoxicity was fully rescued when the concentration of **5** dropped below 10 nM. Remarkably, compared to non-treated NK-92MI cells, NK-92MI-S7$^{high}$ cells modified with 10 nM of **5** exhibited significantly enhanced killing of untrimmed Raji and Daudi cells with their natural sialylation intact (Figure 5c). For example, at the effector-to-target ratio of 5:1, the NK-induced target-cell killing was almost doubled upon $^{FTMC}$Neu5Ac installation. Consistently, the cytotoxicity of peripheral NK cells and the fluorescence activated cell sorting (FACS)-isolated Siglec-7 positive peripheral NK cells was also significantly improved upon ST6Gal1-mediated glycan editing with 10 nM of **5** (Figure 5e and Supplementary figure s12).

When Siglec-expressing immune cells encounter their target cells, binding to the *trans* ligands that are expressed on target cells recruits Siglecs to the immune synapse, where their ITIMs are phosphorylated by Src kinases that are activated due to activation receptor-ligand ligation, thereby creating a binding site for the tyrosine phosphatases SHP-1 and SHP-2. Binding of SHP-1/2 leads to de-phosphorylation of signaling components of activatory receptor to suppress immune cell activation and effector function. Consistent with decreased NK cytotoxicity triggered by the functionalization with high concentrations of **5**, enhanced phosphorylation of Siglec-7 was detected, which was accompanied with an increased SHP-1 recruitment (Figure 5d). On the other hand, when NK cells were functionalized with a low concentration of **5** (i.e. 10 nM), significantly reduced phosphorylation of Siglec-7 and SHP-1 recruitment was observed. Simultaneously, a dramatically decreased Siglec-7 expression level was unexpectedly detected in NK cells (Figure 5d).

**Newly created ligands Modulate Siglec-7 stability on NK cells**

To investigate the mechanism through which high-affinity ligands installed in *cis* on NK cells modulate Siglec-7 inhibitory signaling, we first imaged Siglec-7 distribution on the cell surface of NK-92MI-S7$^{high}$ cells using fluorescence microscopy. As is known for Siglec-2 (CD22) on B cells,[34] in the absence of *trans*-ligands, Siglec-7 formed abundant clusters on NK-92MI-S7$^{high}$ cells (Figure 6a, 1$^{st}$ panel and Supplementary figure s13-15). After removal of cell-surface sialic acid by neuraminidase, Siglec-7 clusters broke up (Supplementary figure s13). As expected, when NK-92MI-S7$^{high}$ cells encountered target Raji cells, Siglec-7 was recruited to the E/T interface (Figure 6a, 1$^{st}$ panel).

Installation of $^{FTMC}$Neu5Ac onto the cell surface of NK-92MI-S7$^{high}$ also induced Siglec-7 cluster formation in a dose-dependent manner (Supplementary figure s15). Not only could these clusters be clearly observed on the modified NK cells that were cultured by themselves, but also on the modified NK cells cultured with Raji cells but without direct contact with Raji. Interestingly, upon Raji cell encountering, a dramatic decrease of cell-surface Siglec-7 was detected on NK-92MI-S7$^{high}$ cells that had been modified with 10 nM of **5**, whereas no significant changes of Siglec-7 were observed on NK-92MI-S7$^{high}$ cells that had been modified with >100 nM CMP-$^{FTMC}$Neu5Ac (shown in the 2$^{rd}$ and 3$^{th}$ panel of Figure 6a)

Consistent with what was observed by imaging, flow cytometry analysis revealed a dramatic decrease (approximately 20–30%) of the Siglec-7 positive NK cell population following the incubation of target cells with NK-92MI-S7$^{high}$ cells that had been modified with 10 nM of **5** (Figure 6b). Similarly, when encountering with target cells, the Siglec-7 positive subset was decreased among periphery NK cells and the sorted Siglec-7 positive periphery NK cells that were functionalized with low levels of $^{FTMC}$Neu5Ac (Figure 6c-e). Surprisingly, no notable increase of Siglec-7 endocytosis was detected as revealed by the weak intracellular Siglec-7 signal. Down-regulation of Siglec-7 expression levels in NK cells (Figure 5d and 6a), coupled with negligible changes in Siglec-7 endocytosis, prompted us to explore the possibility of Siglec-7 release from the plasma membrane. Western blot analysis of Siglec-7 in the culture supernatant revealed that compared to the co-culture supernatant of Raji and un-modified NK-92MI, a dramatically increase of Siglec-7 was detected in the co-culture supernatant of Raji and NK-92MI-modified with 10 nM of **5** (Figure 6f), indicating Siglec-7 was released from NK plasma membrane upon target cell encountering, a process significantly exacerbated by the installation of super-low levels of $^{FTMC}$Neu5Ac.

**Conclusion and Discussion**

Tumor escape from immune-mediated destruction has been associated with mechanisms that suppress immune system effector functions and trigger immune cell exhaustion.[1-3,35,36] The Siglec-sialylated glycan interaction is a newly added member of tumor immune escape pathways.[4-8,11-14] However, the mechanism of this interaction-mediated suppression of anti-tumor immunity is not well understood. Analogous to what has been confirmed for the up-regulated expression of PD-L1 in the tumor microenvironment, which is driven by IFN-γ produced by tumor-infiltrating CD8$^{+}$ T cells,[37] here, we found that encountering with NK cells triggered un-regulation of Siglec-7 ligands on tumor cells. Therefore, contrary to initial preconceptions of tumor-intrinsic high expression

of Siglec-7 ligands, our data argue that tumor cells up-regulate sialylated glycans, which counteracts NK-induced killing via the Siglec-sialylated glycan interaction, a mechanism that is intrinsic to the immune system, and likely represents a physiologic negative feedback loop.

Via ST6Gal1-mediated cell-surface glycan editing, we discovered that a high-affinity and specific ligand of Siglec-7 can be created on NK cells to modulate Siglec-7 signaling and NK effector function. With high levels of the ligand added onto the NK cell surface, enhanced phosphorylation of Siglec-7 and recruitment of SHP-1 was observed, which in turn suppressed the NK-induced target tumor cell killing. On the other hand, at low levels the same ligand induced the release of Siglec-7 from the NK cell surface to the culture medium, which completely reinstalled NK cytotoxicity. We confirmed that the ligand-triggered Siglec-7 secretion only took place after target cell encountering but not by ligand installation itself. Although chronic HIV infection is known to increase plasma levels of a soluble form of Siglec-7,[38] to our knowledge, what observed here is the first case that a high-affinity ligand induces the release of Siglec-7 from NK cell surface. It would be interesting to explore whether it is a common phenomenon that functionalizing immune cells with low levels of high-affinity Siglec-ligands would release Siglecs from the cell surface. If so, this strategy may serve as a general approach to down-regulate Siglecs' inhibitory functions. In this endeavor, we have already demonstrated that high-affinity and specific ligands for other Siglecs, such as Siglec-9[8,28,39], can be introduced onto live cells by employing similar strategies (Supplementary figure s17 and s19).

**Acknowledgment**
This work was supported by the NIH (AI143884 and GM113046 to P.W., P41GM103390, P01GM107012, and R01GM130915 to K.W.M., R01AI050143, P01HL107151, and U19AI136443 to J.C.P.). Prof. M.S.M. would like to thank NSERC, Canada Research Chairs, and the Canadian Glycomics Network for funding. We would like to thank Prof. Mike Boyce for insightful discussions.

**References**

(1) Miller, J. F.; Sadelain, M. The journey from discoveries in fundamental immunology to cancer immunotherapy. *Cancer Cell* **2015**, *27*, 439–449.
(2) Ribas, A.; Wolchok, J. D. Cancer immunotherapy using checkpoint blockade. *Science* **2018**, *359*, 1350–1355.
(3) Sharma, P.; Allison, J. P. The future of immune checkpoint therapy. *Science.* **2015**, *348*, 56–61.
(4) Barkal, A. A. *et al*. CD24 signalling through macrophage Siglec-10 is a target for cancer immunotherapy, *Nature* **2019**, *572*, 392–396.
(5) Wang, J. *et al*. Siglec-15 as an immune suppressor and potential target for normalization cancer immunotherapy, *Nat. Med.* **2019**, *25*, 656–666.
(6) Jandus, C. *et al*. Interactions between Siglec-7/9 receptors and ligands influence NK cell–dependent tumor immunosurveillance, *J. Clin. Invest.* **2014**, *124*, 1810–1820.
(7) Hudak, J. E.; Canham, S. M.; Bertozzi, C. R. Glycocalyx engineering reveals a Siglec-based mechanism for NK cell immunoevasion, *Nat. Chem. Biol.* **2014**, *10*, 69–75.
(8) Macauley, M. S.; Crocker, P. R.; Paulson, J. C. Siglec-mediated regulation of immune cell function in disease, *Nat. Rev. Immunol.* **2014**, *14*, 653–666
(9) Ikehara, Y.; Ikehara, S. K.; Paulson, J. C. Negative regulation of T cell receptor signaling by Siglec-7 (p70/AIRM) and Siglec-9, *J. Biol. Chem.* **2004**, *279*, 43117–43125.
(10) Kawasaki, Y. *et al*. Ganglioside DSGb5, preferred ligand for Siglec-7, inhibits NK cell cytotoxicity against renal cell carcinoma cells. *Glycobiology* **2010**, *20*, 1373–1379.
(11) Tao, L.; Wang, S.; Yang, L.; Jiang, L.; Li, J.; Wang, X. Reduced Siglec-7 expression on NK cells predicts NK cell dysfunction in primary hepatocellular carcinoma, *Clin. Exp. Immunol*. **2020,** DOI: 10.1111/cei.13444
(12) Laubli, H. *et al*. Engagement of myelomonocytic Siglecs by tumor-associated ligands modulates the innate immune response to cancer. *Proc. Natl. Acad. Sci. USA* **2014**, *111*, 14211–14216.
(13) Adams, O. J.; Stanczak, M. A.; von Gunten, S.; Läubli, H., Targeting sialic acid–Siglec interactions to reverse immune suppression in cancer. *Glycobiology* **2018**, *28*, 640–647.

(14) Bornhofft, K. F.; Goldammer, T.; Rebl, A.; Galuska, S. P., Siglecs: A journey through the evolution of sialic acid-binding immunoglobulin-type lectins. *Dev. Comp. Immunol.* **2018**, *86*, 219–231.
(15) Vivier, E. *et al*. Innate or adaptive immunity? The example of natural killer cells. *Science* **2011**, *331*, 44–49.
(16) Veluchamy, J. P. *et al*. The Rise of Allogeneic Natural Killer Cells As a Platform for Cancer Immunotherapy: Recent Innovations and Future Developments. *Frontiers in immunology* **2017**, *8*, 631.
(17) Suck, G. *et al*. NK-92: an 'off-the-shelf therapeutic' for adoptive natural killer cell-based cancer immunotherapy. Cancer Immunol. Immunother. **2016**, *65*, 485–492.
(18) Zhu, L. *et al*. Natural Killer Cell (NK-92MI)-Based Therapy for Pulmonary Metastasis of Anaplastic Thyroid Cancer in a Nude Mouse Model. *Frontiers in immunology* **2017**, *8*, 816.
(19) Hydes, T. et al. IL-12 and IL-15 induce the expression of CXCR6 and CD49a on peripheral natural killer cells. *Immun. Inflamm. Dis.* **2018**, *6*, 34–46.
(20) Carson, W. E. *et al*, Interleukin (IL) 15 is a novel cytokine that activates human natural killer cells via components of the IL-2 receptor. *J. Exp. Med.* **1994**, *180*, 1395–1403.
(21) Gong, J. H.; Maki, G.; Hlingemann, H. G. Characterization of a Human Cell Line (NK-92) With Phenotypical and Functional Characteristics of Activated Natural Killer Cells. *Leukemia* **1994,** *8*, 652–658.
(22) Wratil, P. R. et al. Metabolic glycoengineering with N-acyl side chain modified mannosamines, *Angew Chem. Int. Ed. Engl.* **2016**, *55*, 9482–9512.
(23) Wang, W. *et al.* Sulfated ligands for the copper(I)-catalyzed azide-alkyne cycloaddition. *Chem. Asian J.* **2011,** *6*, 2796–2802.
(24) Donaldson, J. G.; Finazzi, D.; Klausner, R. D. Brefeldin A inhibits Golgi membrane-catalysed exchange of guanine nucleotide onto ARF protein, *Nature* **1992**, 360, 350–352.
(25) Macia, E.; Ehrlich, M.; Massol, R.; Boucrot, E.; Brunner, C.; Kirchhausen, T. Dynasore, a cell-permeable inhibitor of dynamin. *Dev. Cell* **2006**,10, 839–850.
(26) Avril, T.; North, S. J.; Haslam, S. M.; Willison, H. J.; Crocker, P. R. Probing the cis interactions of the inhibitory receptor Siglec-7 with alpha2,8-disialylated ligands on natural killer cells and other leukocytes using glycan-specific antibodies and by analysis of alpha2,8-sialyltransferase gene expression. *J. Leukoc. Biol.* **2006**, *80*, 787–796.
(27) Nicoll, G.; Avril, T.; Lock, K.; Furukawa, K.; Bovin, N.; Crocker, P. R. Ganglioside GD3 expression on target cells can modulate NK cell cytotoxicity via siglec-7-dependent and -independent mechanisms. *Eur. J. Immunol.* **2003**, *33*, 1642–1648.
(28) Rillahan, C. D. *et al*. On-chip synthesis and screening of a sialoside library yields a high affinity ligand for Siglec-7. *ACS Chem. Biol.* **2013**, *8*, 1417–1422.
(29) Sugiarto, G. et al. A sialyltransferase mutant with decreased donor hydrolysis and reduced sialidase activities for directly sialylating LewisX. *ACS Chem. Biol.*. **2012**, *7*, 1232–1240.
(30) Briard, J. G., Jiang, H., Moremen, K. W., Macauley, M. S.; Wu, P. Cell-based glycan arrays for probing glycan-glycan binding protein interactions. *Nat. Commun.* **2018**, 9, 880–890.
(31) Patnaik, S. K.; Stanley, P. Lectin-resistant CHO glycosylation mutants. *Methods Enzymol.* **2006**, *416*, 159–182.
(32) Aguilar, A. L.; Briard, J. G.; Yang, L.; Ovryn, B.; Macauley, M. S.; Wu, P. Tools for studying glycans: recent advances in chemoenzymatic glycan labeling. *ACS Chem. Biol*. **2017**, 12, 611–621.
(33) Moremen, K. W. et al. Expression system for structural and functional studies of human glycosylation enzymes. *Nat. Chem. Biol*. **2018**, 14, 156–162.
(34) Collins, B. E.; Smith, B. A.; Bengtson, P.; Paulson, J. C. Ablation of CD22 in ligand-deficient mice restores B cell receptor signaling. *Nat. Immunol*. **2006**, 7, 199–206.
(35) Wherry, E. J.; Kurachi, M. Molecular and cellular insights into T cell exhaustion. *Nat. Rev. Immunol*. **2015**, *15*, 486–499.
(36) Blank, C. U. *et al*. Defining 'T cell exhaustion'. *Nat. Rev.Immunol.* **2019**, *19*, 665–674.
(37) Spranger, S. *et al*. Up-regulation of PD-L1, IDO, and $T_{regs}$ in the melanoma tumor microenvironment is driven by $CD8^+$ T cells. *Sci. Trans. Med*. **2013**, 5, 200ra116.
(38) Varchetta, S. *et al.* Lack of Siglec-7 expression identifies a dysfunctional natural killer cell subset associated with liver inflammation and fibrosis in chronic HCV infection. *Gut*, **2015**, 0, 1–9.

(39) Rillahan, C. D.; Schwartz, E.; McBride, R.; Fokin, V. V.; Paulson, J. C. Click and pick: identification of sialoside analogues for siglec-based cell targeting. *Angew Chem. Int. Ed. Engl.* **2012**, *51*, 11014–11018.

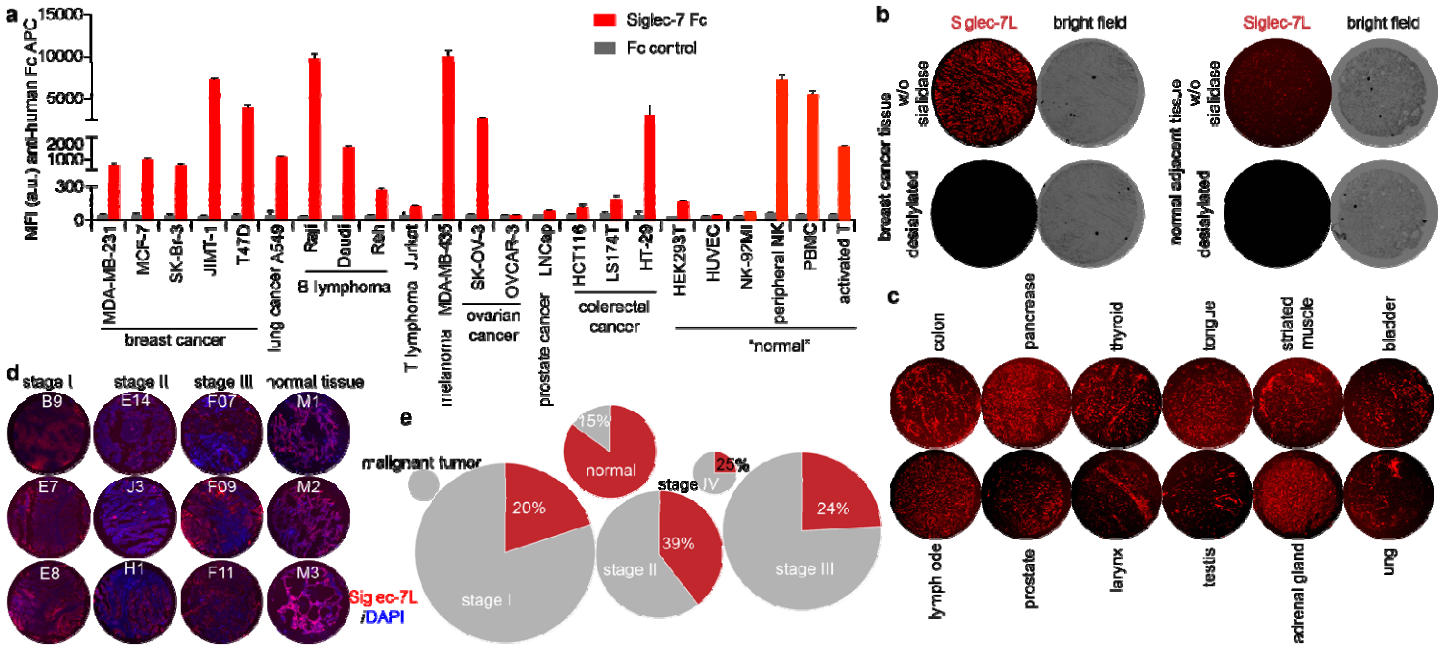


Figure 1. Profile Siglec-7 ligand (Sigle-7L) expression on the cell surface of live cells and human tissue specimens.

(a) Cell lines and primary immune cells from healthy human donors were stained with recombinant Siglec-7 Fc pre-complexed with an anti-human Fc-APC antibody, and the Fc was used as control for ligand-specificity. Error bar represents the standard deviation of three biological samples. (b) Probe the Siglec-7L expression in human breast cancer tissues and the normal adjacent tissues that were pretreated with sialidase to remove sialic acids or not. (c) Probe the Siglec-7L expression in different human malignant tissues. (d and e) Probe the Siglec-7L expression in lung cancer tissues and normal tissues from different donors (total 197 samples). The lung malignant tumor samples (n=2), stage I lung malignant (n=75), stage II lung malignant (n=38), stage III lung malignant (n=58), stage IV lung malignant (n=4), and normal lung tissue (n=20) were implied for Siglec-7L screening, and sample volume in each group was plotted as circle area (e). Low (gray) and high (red) Siglec-7L levels were classified based on Siglec-7 Fc staining fluorescence intensity, and the relative ratio of high Siglec-7L specimen was listed out as % percentages. Three of presentative Siglec-7L-high samples were presented (right panel).

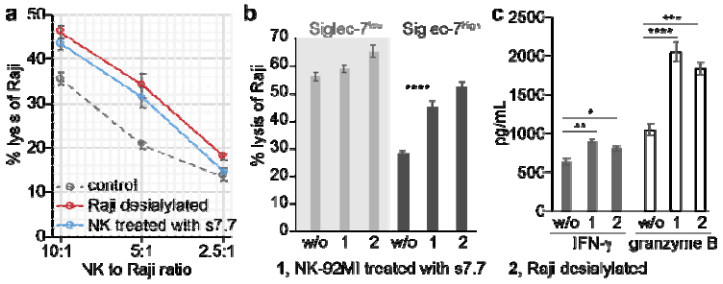


**Figure 2.** The cytotoxicity of NK cells were impaired by 'Sialic acid-Siglec-7' interactions.
(a and b) LDH release assay for quantifying the cytotoxicity of the periphery NK cells (a) and NK-92MI (b) against Raji cells. The pre-desialylation of Raji cells were conducted by treating with sialidase. The anti-Siglec-7 antibody (clone s7.7) blocking was performed before co-incubation of NK with Raji cells. (c) ELISA quantification of IFN-λ and granzyme B produced by NK-92MI-S7$^{high}$ cells after incubation with Raji cells for 1h at an E/T ratio of 5:1. The bars represent standard error of three biological replicates. The significance was analyzed with the two-sided Students t-test. Note, *, p<0.05; **, p<0.01; ***, p<0.005; ****, p<0.001.

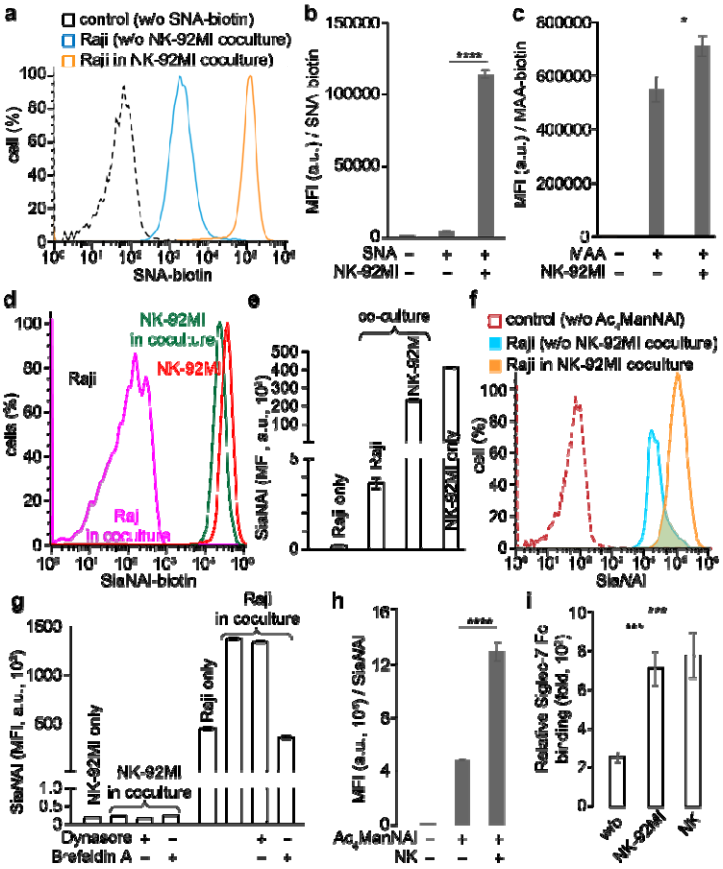


**Figure 3.** Interactions between NK and Raji cells leads to an upregulation of Siglec-7 ligands on Raji cells
(a) SNA lectin staining of α2-6-sialic acids on Raji cells. (b and c) Mean fluorescence intensity (MFI) of SNA (b) and MAA (c) lectin staining of Raji cells. (d and e) transferring of SiaNAl-labeled sialosides from NK-92MI cells to Raji cells upon co-culture of both cells. (f and g) $Ac_4$ManNAl-based metabolic glycan labeling of Raji cells in the coculture with NK-92MI-S7 cells, in the presence of dynasore, brefeldin A, or not. (h) Coculture with periphery NK cells also significantly induced Raji cells to express higher sialylation level, as revealed by $Ac_4$ManNAl-labeling. (i) NK-induced up-regelation of sialylation on Raji cells further significantly increased the binding of Siglec-7 Fc. In Figure b, c, e, and g-I, the bars represent standard error of the MFI of three biological repeats of samples. The significance was analyzed with the two-sided Students t-test. Note, *, p<0.05; ***, p<0.005; ****, p<0.001.

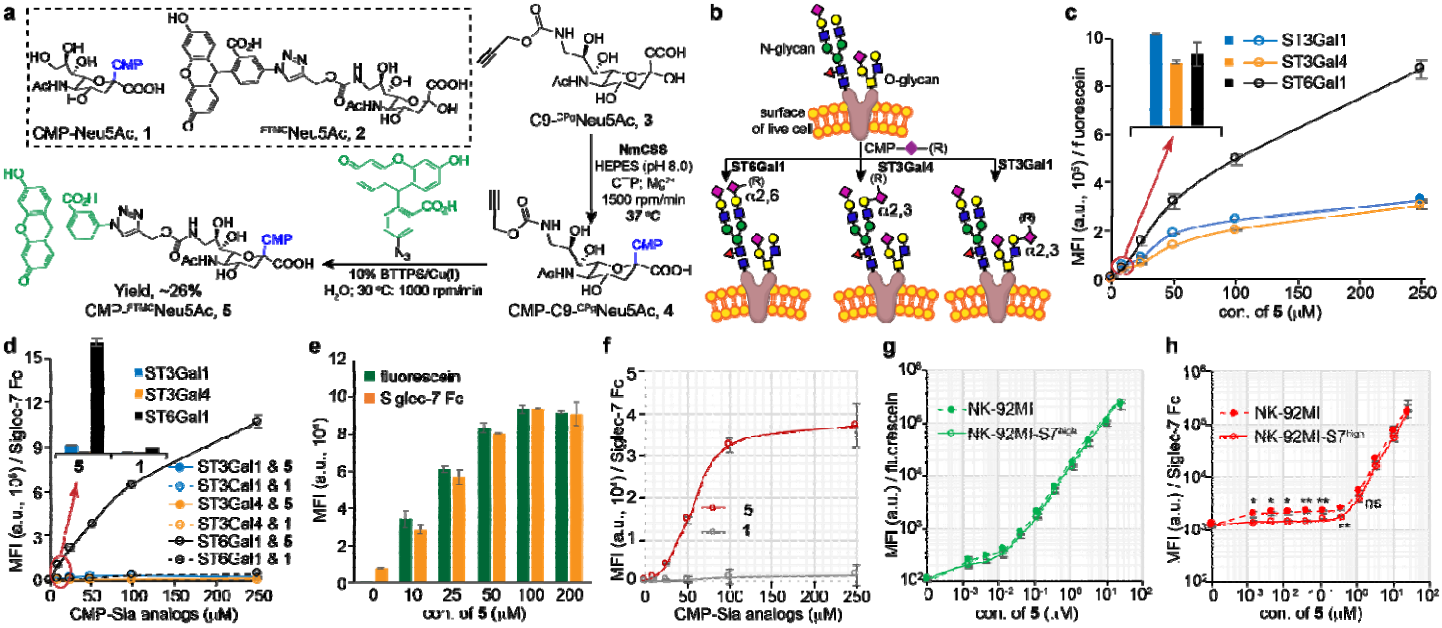


**Figure 4**. ST-assisted *in situ* creation of Siglec-7 high-affinity ligands on live cells.
(a) One-pot synthesis of CMP-$^{FTMC}$Neu5Ac (**5**). (b) Workflow for ST-mediated glycan editing. (c and d) STs-assisted incorporation of $^{FTMC}$Neu5Ac onto the Lec2 cells was probed with the resultant fluorescein signals (c) and Siglec-7 Fc binding (d). (e) ST6Gal1-assisted incorporation of $^{FTMC}$Neu5Ac onto the periphery NK cells was probed with the resultant fluorescein signals and Siglec-7 Fc binding. (f) ST6Gal1-assisted incorporation of $^{TMC}$Neu5Ac or natural Neu5Ac onto NK-92MI cells was probed by Siglec-7 Fc. (g and h) ST6Gal1-assisted incorporation of $^{FTMC}$Neu5Ac onto the NK-92MI or NK-92MI-S7$^{high}$ cells was probed with the resultant fluorescein signals (g) and Siglec-7 Fc binding (h). In Figure c-h, the bars represent standard error of three biological repeats of samples. The significance was analyzed with the two-sided Students t-test. Note, ns, not significant; *, $p<0.05$; **, $p<0.01$.

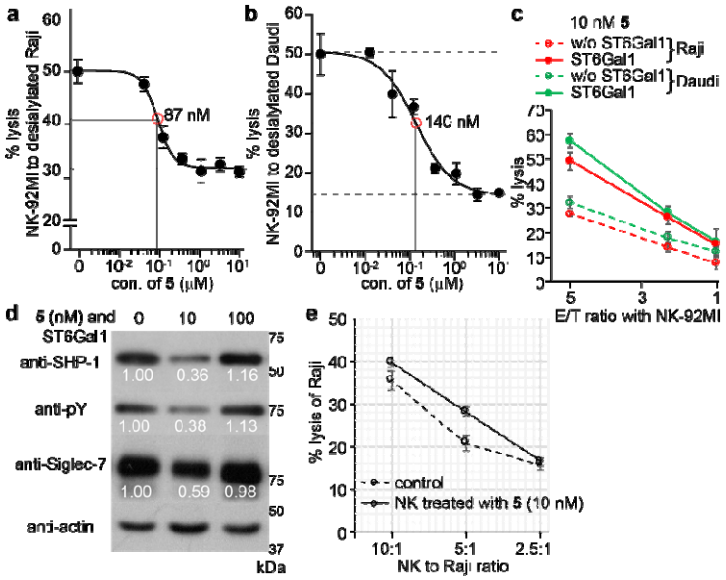


**Figure 5.** NK cell-surface newly created *cis* high-affinity Siglec-7 ligands modulated NK-cytotoxicity against target cells.

(a-c) LDH release assay for quantifying the cytotoxicity of the NK-92MI-S7$^{high}$ cells against Raji (a and c) and Daudi cells (b and c). The NK-92MI-S7$^{high}$ cells with or without $^{FTMC}$Neu5Ac incorporation were used (d) Western blot analysis of Siglec-7 activation. NK-92MI-S7$^{high}$ cells with or without $^{FTMC}$Neu5Ac modification were incubated with Raji cells and lysed, followed by anti-Siglec-7 immunoprecipitation. A decrease in SHP-1 recruitment and Siglec-7 phosphorylation was seen in NK cells after treating with 10 nM of **5** but not 100 nM of **5**. The numbers indicate the relative quantification of binds intensity to that of actin by ImageJ. (e) The specific lysis of Raji using the periphery NK cells with or without $^{FTMC}$Neu5Ac modification. In Figure a-c and e, the bars represent standard error of three biological repeats of samples. The significance was analyzed with the two-sided Students t-test. Note, ns, not significant; *, $p<0.05$; **, $p<0.01$.

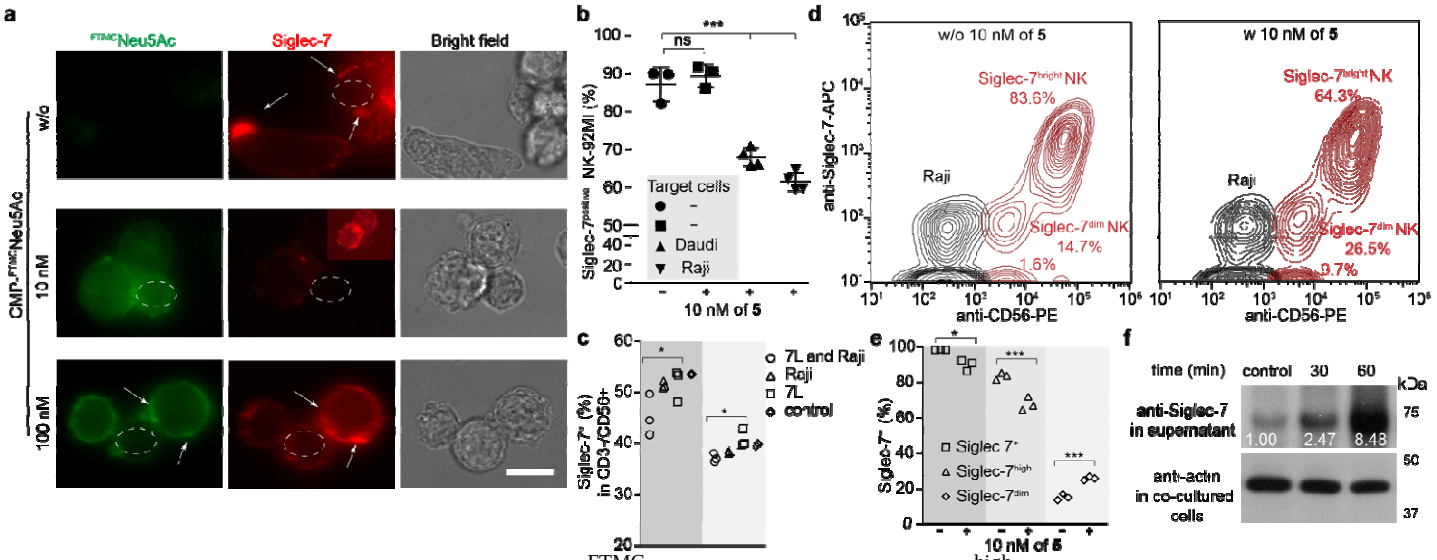


**Figure 6**. ST6Gal1-assisted incorporation of $^{FTMC}$Neu5Ac on NK-92MI-S7$^{high}$ or periphery NK cells modulates Siglec-7 inhibitory signaling.

(a) Fluorescence microscopy images of Siglec-7 on NK-92MI-S7$^{high}$ cells with ST6Gal1 or not. The white dash circles indicate the presence of target cells, the white arrows indicate the identified clusters of Siglec-7 and the purple arrows indicate the *in situ* transfer of ligands (green) to target cells from NK cells. The two white rectangles present the brightened pictures of the same views. Scale bar: 20 μm. (b and c) Siglec-7 positive populations of NK-92MI-S7$^{high}$ cells (b) or periphery NK cells raised from two different healthy donors (c) treated with ST6Gal1-staSE under 10 nM of **5** were counted via flow cytometry. (d and e) The sorted Siglec-7 positive periphery NK cells were treated with10 nM of **5, and then** were cocultured with Raji cells at an E/T ratio of 5:1. (f) Western blot analysis of Siglec-7 released into the supernatant of the coculture of NK-92MI-S7$^{high}$ cells with Raji cells at an E/T ratio of 5:1. The significance was analyzed with the two-sided Students t-test. Note, ns, not significant; *, $p<0.05$; ***, $p<0.005$.